

Effect of the synthesis method of SnSb anode materials on their electrochemical properties

Chaoli Yin, Hailei Zhao, Hong Guo, Xianliang Huang, and Weihua Qiu

Department of Inorganic Nonmetallic Materials, University of Science and Technology Beijing, Beijing 100083, China

(Received 2006-07-28)

Abstract: SnSb alloy powders for the anode of Li-ion batteries were synthesized by two kinds of reduction precipitation methods: solution titration and rapid mixing. Two kinds of SnSb alloy powders showed different phase compositions and particle morphologies although the same starting materials were used. The SnSb alloy electrode synthesized by titration exhibits high reversible specific capacity and good cycling stability, whereas the rapid-mixing sample shows high irreversible capacity and fast capacity fade. The broad particle size distribution of SnSb powders synthesized by titration is considered to be responsible for the improvement of cycling stability. The initial charge-discharge efficiency exceeding 80% has been obtained for the titration sample. The electrochemical reaction process of two kinds of synthesized SnSb composite electrodes was characterized by cyclic voltammetry and AC impedance techniques.

Key words: SnSb alloys; lithium-ion batteries; anode; electrochemical properties

[This study was financially supported by the National Natural Science Foundation of China (No.50371007) and the National High-Tech Research and Development Program of China (863 Program, No.2006AA03Z231).]

1. Introduction

Rechargeable lithium-ion batteries with their light-weight and high energy density have become an important source for powering many applications. Although the performance is excellent, there still is room for improvement, especially in terms of the replacement of conventional electrodes with new materials having enhanced energy content. The specific capacity of carbonaceous anode materials is now much close to its theoretical value, $372 \text{ mAh}\cdot\text{g}^{-1}$ (LiC_6), therefore, the space to further increase its capacity is severely limited. The demand for high-energy density-rechargeable batteries has stimulated the research for new storage electrode materials [1-4].

Various metals and metal oxides, which can reversibly accommodate lithium, have been extensively studied as Li-insertion anodes for lithium-ion batteries because of their high volumetric and mass energy densities. In particular, attention has been focused on some storage metals such as tin, antimony, and silicon that show much higher Li storage capacities than the presently used carbonaceous materials ($\text{Li}_{22}\text{Sn}_5$: $994 \text{ mAh}\cdot\text{g}^{-1}$; Li_3Sb : $660 \text{ mAh}\cdot\text{g}^{-1}$; $\text{Li}_{22}\text{Si}_5$: $4000 \text{ mAh}\cdot\text{g}^{-1}$) [5-6]. However, cycling stability of a metal anode is

often limited by rapid mechanical disintegration due to the drastic volume changes of metallic host matrices upon lithiation and delithiation.

Fortunately, it has been demonstrated by various research groups that the said shortcoming can partly be overcome by adopting multiphase instead of single-phase materials or by using intermetallic compounds [5, 7-14]. In addition, some research work indicated that cycling stability of an alloy anode could be improved by using nanosized active powders and limiting lithium input, which could buffer or restrict the stress changes during cycling [5, 7]. However, small particle size, usually accompanied by large surface area, easily results in high initial irreversible capacity loss due to the reduction of surface contaminants and the formation of solid electrolyte interface (SEI) film.

In this study, SnSb alloy powders for Li-ion batteries were synthesized by reductive precipitation process *via* two methods: rapid mixing proposed by Besenhard and coworkers [10] and solution titration. The particle morphologies and phase compositions of two kinds of synthesized SnSb powders were compared, and the effects of both on the electrochemical properties were investigated.

2. Experimental

Two aqueous solutions were used for the synthesis of SnSb powder, namely, solution A formed by $\text{SnCl}_2 \cdot 2\text{H}_2\text{O}$, $\text{SbCl}_3 \cdot \text{H}_2\text{O}$, and complexant citrates; and solution B formed by NaOH and NaBH_4 . Two different procedures were used to prepare the SnSb alloy powder. One is a titration process in which solution B was slowly titrated into solution A under continuous stirring. The other one follows basically the procedure recommended in Ref. [10], *i.e.* two solutions were mixed rapidly under strong agitation. The precipitation was filtrated and subsequently washed with distilled water, 0.35 M HCl , distilled water, and acetone, followed by drying at 120°C in vacuum. The SnSb powders prepared by solution titration and rapid-mixing methods are referred to as sample (a) and sample (b), respectively. The particle morphologies and phase compositions of the two kinds of synthesized SnSb powders were characterized by scanning electron microscopy (SEM) and X-ray diffraction (XRD), respectively.

The composite electrodes were prepared by pasting a slurry containing 75wt% active material (SnSb alloy powders), 13wt% conductive additive (acetylene black), and 12wt% binder polyvinylidene fluoride (PVDF) dissolved in 1-methyl-2-pyrrolidinone (NMP) onto a copper substrate. After predrying at 50°C , the electrodes were pressed and dried in vacuum at 120°C for 2 h. The weight of the composite electrodes was 3-5 mg. The cells were assembled in argon filled glove box. Metallic lithium foil was used as the counter electrode. All cells contained sufficient organic electrolyte of 1 M $\text{LiPF}_6/\text{EC}+\text{DMC}$ (1:1). Celgard 2400 was used as the separator. The cycling tests were carried out at the charge and discharge current density of 100 mA/g in the voltage range of 0.01-1.2 V vs. Li/Li^+ . The capacity of electrodes was calculated on the basis of the weight of active materials. Cyclic

voltammetry (CV) and electrochemical impedance spectroscopy (EIS) were performed on a Chi660a workstation. CV was carried out between 0.01 and 1.6 V with a scan rate of 0.05 mV/s and EIS was run with a frequency range of 100 kHz-10 mHz.

3. Results and discussion

The XRD patterns of SnSb alloy powders synthesized by two different methods are shown in Fig. 1. Peaks specific for SnSb and Sn are detected in both the samples. However, the peaks corresponding to Sb is present in sample (a) but not in sample (b), and the peaks due to Sn are much stronger in sample (a) compared with those in sample (b), indicating the incomplete alloying of Sn with Sb in sample (a). This is probably because of the different reduction sequences of Sn and Sb from corresponding salts in the titration method. In addition, sample (a) shows sharper peaks than those of sample (b), suggesting the high crystallinity and large particle size of sample (a).

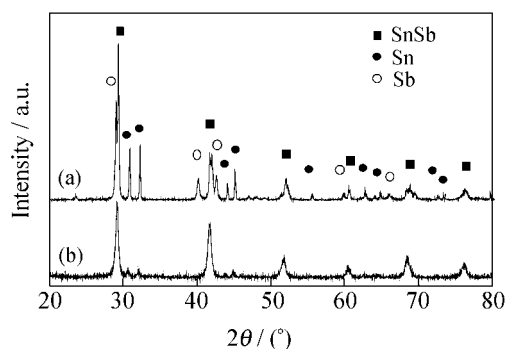


Fig. 1. XRD patterns of SnSb alloy powders prepared by titration (a) and rapid mixing (b).

SEM images (Fig. 2) illustrate the differences in particle morphologies of two kinds of SnSb alloy powders. Sample (a) shows a relatively large average particle size (~ 350 nm) and a wide particle size distribution, whereas single and nanosized particles appear in sample (b).

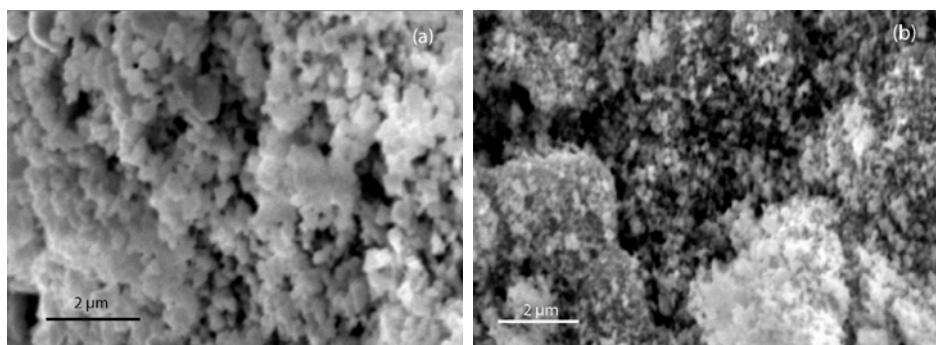


Fig. 2. SEM images of SnSb alloy powders prepared by titration (a) and rapid mixing (b).

Fig. 3 shows the cycle performance of the two samples in terms of the capacity delivered with cycle

number. Sample (a) exhibits a higher specific capacity and a better cycling stability than sample (b). The

charge capacity for sample (a) is more than 550 $\text{mAh}\cdot\text{g}^{-1}$ after 10 cycles, whereas it is 294 $\text{mAh}\cdot\text{g}^{-1}$ for sample (b). This could be attributed to the multiphase characteristic and the good crystallinity of sample (a). Additionally, the randomly distributed particle size in sample (a) may also have the possibility of homogenizing the electrode structure and the mechanical stresses caused by the big volume changes, preventing the cracking of the electrode, and thus improving the cycling performance of the composite electrode. Sample (a) displays a lower initial irreversible capacity than sample (b). The first coulombic efficiencies of two samples are about 80% and 53% for samples (a) and (b), respectively. The possible reason for this difference is directly related to the particle size of synthesized SnSb powders. Sample (a) with relatively large particle size should have lower specific surface area and thus, lower possibility to contact with the electrolyte. Accordingly, the irreversible capacity loss because of the formation of SEI film is decreased. On the other hand, the lower specific surface area usually accompanies the lower impurities, especially the oxides, which is deemed to be the other important origin of the initial irreversible capacity [7-10].

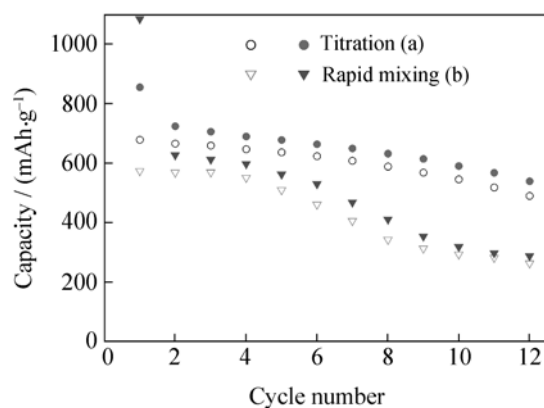


Fig. 3. Cycle performance of SnSb electrodes prepared by titration (a) and rapid mixing (b).

The charge/discharge profiles of the constant current cycling of the SnSb electrodes are shown in Fig. 4. For two samples, the first cycle differs from the next ones, *i.e.* the materials undergo a formation cycle in which the first expansion of the active material and the composite electrode occurs [1, 15]. For sample (b), the first discharge profile exhibits a long slope before the first plateau associated with the formation of Li_3Sb phase. This is mostly ascribed to the oxygen impurity, electrolyte decomposition at the electrode/electrolyte, and to the formation of a protective film because of the larger surface areas of sample (b). The multi-plateau behavior reflects the characteristics of the electrochemical process that is associated with

various lithium-alloying (charge)-lithium-de-alloying (discharge) stages [16]. Compared with sample (a), the multi-plateau characteristic of sample (b) becomes undistinguishable, mainly because of its poor crystallinity of ultrafine powders [8]. With the increased cycles, the profile of sample (a) tends to be smooth, which is brought by the decrease of crystallinity and the pulverization of active powders along with cycling. Two close delithiation plateaus at ~ 1.0 V are observed for sample (a) but only one for sample (b). This means that the delithiation of Li_3Sb phase may be a two-step process in the SnSb electrode of sample (a).

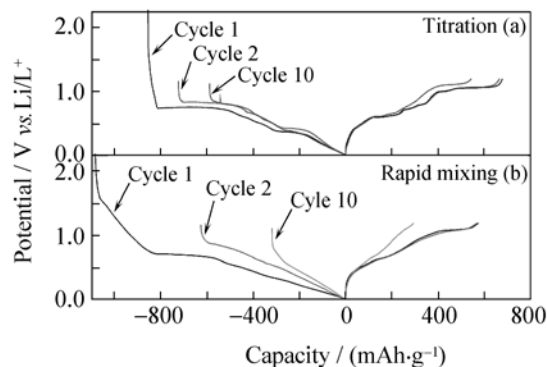


Fig. 4. Charge-discharge profiles of SnSb electrodes prepared by titration (a) and rapid mixing (b).

CV profiles of the two samples after two cycles are shown in Fig. 5. In the CVs of sample (a), five distinct peaks are observed during the cathodic and the anodic scans, which are ascribed to the reactions of both phases SnSb and Sb to Li_3Sb and Sn, and the reaction of Sn (including the original Sn and newly formed Sn) to various lithiated Sn phases. However, only two broad peaks are found in the CVs of sample (b). This result is consistent with the undistinguishable plateau characteristic of sample (b) shown in Fig. 4. One peak at 0.78 V vs. Li/Li^+ corresponds to the reaction of phase SnSb to Li_3Sb and Sn. The other peaks below 0.5 V vs. Li/Li^+ represents these reactions of phase Sn (mostly newly formed Sn) to various lithiated Sn phases, which occur one after the other. In addition, an interesting feature can be noticed. For sample (a), the anodic peak at ~ 1.15 V exhibits a shoulder at the lower potential side, which also indicates the two steps delithiation process of Li_3Sb [8].

Fig. 6 shows the impedance response of the two samples in this study. The response is qualitatively similar for the two samples. Both curves can be divided into four segments which represent the following: (i) resistance contribution from the electrolyte and cell components, (ii) the resistive and capacitive contribution arising from the surface film, (iii) the charge-transfer resistance, and (iv) the Warburg contribution.

There are, however, some significant differences in the width of both semicircles (ii and iii), and in the trend of the low-frequency Warburg lines (iv). The width of both semicircles of sample (a) is smaller than that of sample (b), which indicates the lower electrochemical impedance of sample (a). The large amount of SEI film produced on the electrode surface of sample (b) may have strong impact on the electrochemical impedance of SnSb electrode. The difference in the trend of low-frequency Warburg line can be related to the diffusion rate of Li^+ and the accumulation of Li^+ in the two anode materials [17-18]. The above information indicates the lower electrochemical impedance and the faster kinetics of sample (a) than those of sample (b).

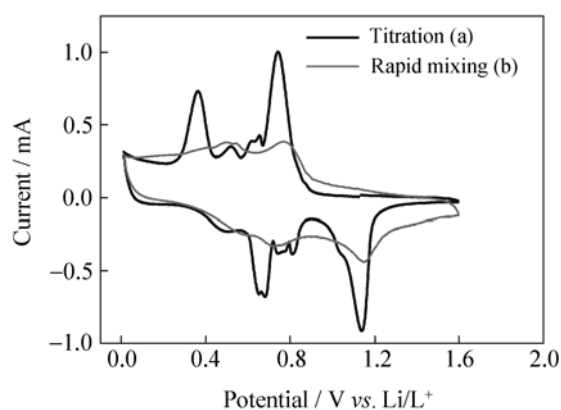


Fig. 5. Cyclic voltammety of the composite electrodes prepared by titration (a) and rapid mixing (b).

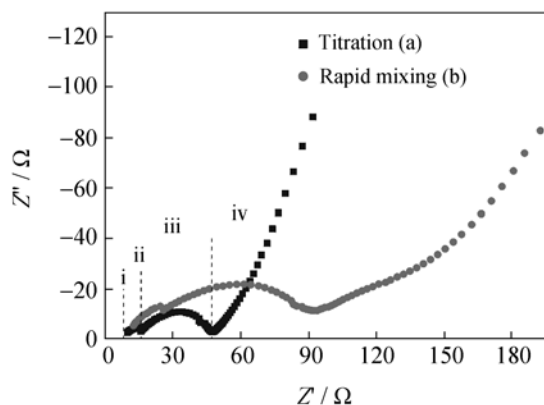


Fig. 6. Impedance spectra of the composite electrodes prepared by titration (a) and rapid mixing (b).

4. Conclusions

In this study, SnSb alloy powders for the anode of Li-ion batteries were synthesized by two kinds of reduction precipitation methods: solution titration and rapid mixing. The former gave a relatively large particle size with broad size distribution and multiphase composition, whereas the latter produced a single SnSb phase with nanosized particles, although the same starting materials were used. The titration sam-

ple showed a high reversible specific capacity and good cycling stability than the rapid-mixing sample. Moreover, a high initial coulombic efficiency, exceeding 80% for the titration sample, has rarely been reported for similar materials. The titration sample displayed multi-CV peaks and less electrochemical impedance compared with the rapid-mixing sample.

References

- [1] J. Yang, M. Winter, and J.O. Besenhard, Small particle size multiphase Li-alloy anodes for lithium-ion batteries, *Solid State Ionics*, 90(1996), p.281.
- [2] H. Zhao, D.H.L. Ng, Z. Lu, and N. Ma, Carbothermal synthesis of Sn_xSb anode material for secondary lithium-ion battery, *J. Alloys Compd.*, 395(2005), p.192.
- [3] O. Crosnier, T. Brousse, X. Devaux, P. Fragnaud, and D.M. Schleich, New anode systems for lithium ion cells, *J. Power Sources*, 94(2001), p.169.
- [4] Y.L. Kin, S.J. Lee, H.K. Baik, S.M. Lee, Sn-Zr-Ag alloy thin-film anodes, *J. Power Sources*, 119-121(2003), p.106.
- [5] J. Yang, Y. Takeda, N. Imanishi, and O. Yamamoto, Ultrafine Sn and $\text{SnSb}_{0.14}$ powders for lithium storage materials in lithium-ion batteries, *J. Electrochem. Soc.*, 146(1999), p.4009.
- [6] S. Bourderau, T. Brousse, and D.M. Schleich, Amorphous silicon as a possible anode material for Li-ion batteries, *J. Power Sources*, 81-82(1999), p.233.
- [7] J. Yang, Y. Takeka, N. Imanishi, T. Ichikawa, and O. Yamamoto, SnSb_x -based composite electrodes for lithium ion cells, *Solid State Ionics*, 135(2000), p.175.
- [8] M. Wachtler, M. Winter, and J.O. Besenhard, Anodic materials for rechargeable Li-batteries, *J. Powder Sources*, 105(2002), p.151.
- [9] M. Wachtler, J.O. Besenhard, and M. Winter, Tin and tin-based intermetallics as new anode materials for lithium-ion cells, *J. Power Sources*, 94(2001), p.189.
- [10] J. Yang, M. Wachtler, M. Winter, and J.O. Besenhard, Sub-microcrystalline Sn and Sn-SnSb powders as lithium storage materials for lithium-ion batteries, *Electrochem. Solid State Lett.*, 2(1999), p.161.
- [11] M. Winter and J.O. Besenhard, Electrochemical lithiation of tin and tin-based intermetallics and composites, *Electrochim. Acta*, 45(1999), p.31.
- [12] D.G. Kim, H. Kim, H.J. Sohn, T. Kang, Nanosized Sn-Cu-B alloy anode prepared by chemical reduction for secondary lithium batteries, *J. Powder Sources*, 104(2002), p.221.
- [13] J. Wolfenstine, S. Campos, D. Foster, J. Read, and W.K. Bohl, Nano-scale Cu_6Sn_5 anodes, *J. Powder Sources*, 109(2002), p.230.
- [14] O. Mao, R.A. Dunlap, and J.R. Dahn, Mechanically alloyed Sn-Fe(-C) powders as anode materials for Li-ion batteries, *J. Electrochem. Soc.*, 146(1999), p.405.
- [15] M. Wachtler, M.R. Wagner, M. Schmied, M. Winter, and J.O. Besenhard, The effect of the binder morphology on the cycling stability of Li-alloy composite electrodes, *J. Electroanal. Chem.*, 510(2001), p.12.
- [16] H. Mukaibo, T. Osaka, P. Reale, S. Panero, B. Scrosati,

- and M. Wachtler, Optimized Sn/SnSb lithium storage materials, *J. Power Sources*, 132(2004), p.225.
- [17] K.M. Shaju, G.V. Subba Rao, and B.V.R. Chowdari, Influence of Li-ion kinetics in the cathodic performance of layered Li (Ni_{1/3}Co_{1/3}Mn_{1/3})O₂, *J. Electrochem. Soc.*, 151(2004), p.A1324.
- [18] D. Aurbach, Review of selected electrode-solution interactions which determine the performance of Li and Li ion batteries, *J. Power Sources*, 89(2000), p.206.